Efficient Computation of Multiple Density-Based Clustering Hierarchies

Antonio Cavalcante Araujo Neto[†], Joerg Sander[†], Ricardo J. G. B. Campello[‡], and Mario A. Nascimento[†]

[†]Department of Computing Science, University of Alberta, Canada

[‡]College of Science and Engineering, James Cook University, Australia

{antonio.cavalcante, jsander, mario.nascimento}@ualberta.ca[†], ricardo.campello@jcu.edu.au[‡]

Abstract—HDBSCAN*, a state-of-the-art density-based hierarchical clustering method, produces a hierarchical organization of clusters in a dataset w.r.t. a parameter $mpts$. While the performance of HDBSCAN* is robust w.r.t. $mpts$ in the sense that a small change in $mpts$ typically leads to only a small or no change in the clustering structure, choosing a "good" $mpts$ value can be challenging: depending on the data distribution, a high or low value for $mpts$ may be more appropriate, and certain data clusters may reveal themselves at different values of $mpts$. To explore results for a range of $mpts$ values, however, one has to run HDBSCAN* for each value in the range independently, which is computationally inefficient. In this paper, we propose an efficient approach to compute all HDBSCAN* hierarchies for a range of $mpts$ values by replacing the graph used by HDBSCAN* with a much smaller graph that is guaranteed to contain the required information. An extensive experimental evaluation shows that with our approach one can obtain over one hundred hierarchies for the computational cost equivalent to running HDBSCAN* about 2 times.

I. INTRODUCTION

The discovery of groups within datasets plays an important role in the exploration and analysis of data. For scenarios where there is little to no prior knowledge about the data, clustering techniques are widely used. Density-based clustering, in particular, is a popular clustering paradigm that defines clusters as high-density regions in the data space, separated by low-density regions. Algorithms in this class, such as DBSCAN [10], DENCLUE [14], OPTICS [2] and HDBSCAN* [6], stand out for their ability to find clusters of arbitrary shapes and to differentiate between cluster points and noise.

HDBSCAN*, the current state-of-the-art, computes a *hierarchy* of nested clusters, representing clusters at different density levels. It generalizes and improves several aspects of previous algorithms, and allows for a comprehensive framework for cluster analysis, visualization, and unsupervised outlier detection [6]. It requires a single parameter $mpts$, a smoothing factor that can implicitly influence which clusters are detectable in the cluster hierarchy. Choosing a "correct" value for $mpts$ is typically not trivial. For instance, consider the examples in Figure 1, which shows the results of HDBSCAN* (with automatic cluster extraction) for two datasets A and B and two sample $mpts$ values, $mpts = 5$ and 25, selected after running HDBSCAN* multiple times to both datasets w.r.t. $mpts \in \{2, 3, ..., 100\}$. The main points here is that (1) there is no single value of $mpts$ that would result in the extraction of the clusters in both cases, and (2) a

user would not know for a general dataset which value for $mpts$ is suitable. Dataset A is completely labeled as noise for $mpts > 24$, while the two structures in dataset B only start to be detected as separate clusters for $mpts > 24$. It may even be the case that different values of $mpts$ are needed to reveal clusters in different areas of the data space of a single dataset.

To analyze clustering structures in practice, users typically run HDBSCAN* (like other algorithms with a parameter) multiple times with several different $mpts$ values, and explore the resulting hierarchies. Ideally, one would want to analyze cluster structures w.r.t. a large range of $mpts$ values, to fully explore a dataset in a given application. A larger range of HDBSCAN* solutions for a multiple values of $mpts$ values offers greater insight into a dataset, also providing additional opportunities for exploratory data analysis. For instance, using internal cluster validation measures such as DBCV [21], one can identify promising density levels from different hierarchies, produced from different tunings of the algorithm's density estimates (based on $mpts$).

However, one is typically constrained by the required runtime for running HDBSCAN* once for each desired value of $mpts$, resulting from the fact that HDBSCAN* is based on computing a Minimum Spanning Tree (MST) for a *complete* graph, for a given value of $mpts$. Even though this complete graph does not need to be explicitly stored, it has $O(n^2)$ edges (for n data points) whose weights depend on $mpts$. For each desired value of $mpts$, these weights have to be re-computed and an MST has to be constructed for the corresponding complete graph. We note that the computational cost for the MST construction depends on the number of edges in the input graph, $O(n^2)$ in this case.

As the main contribution in this paper we provide theoretical and practical results that lead us to a method for computing multiple hierarchies w.r.t a range of $mpts$ values $(k_1, \ldots, k_{max})$, which is much more efficient than re-running HDBSCAN* for each $mpts$ in this range. This gives access to a large range of HDBSCAN* solutions for a low computational cost, in fact equivalent to the cost of running HDBSCAN* for only 1 or 2 values of $mpts$. To achieve that, we show the following:

1) The smallest known neighborhood graph that contains the Euclidean Minimum Spanning Tree (EMST) is the relative neighborhood graph (RNG) — as a first step towards finding a small, single spanning subgraph that
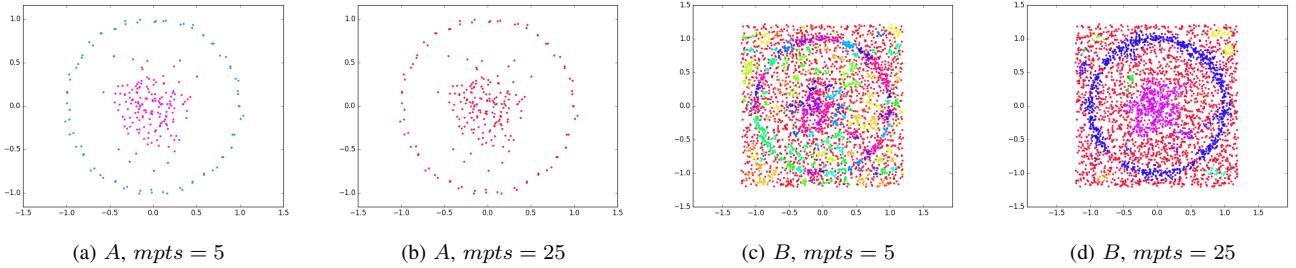
| (a) A, $mpts = 5$ | (b) A, $mpts = 25$ | (c) B, $mpts = 5$ | (d) B, $mpts = 25$ |

Fig. 1: Clusters from datasets A and B for $mpts = 5$ and 25. Noise points are colored in red in all plots.

can replace the complete graph in HDBSCAN*, while maintaining HDBSCAN*'s correctness.

2) The proximity measure used in HDBSCAN*, which depends on $mpts$, can be used to define RNGs that can replace the complete graph in HDBSCAN* with a corresponding RNG, one for each value of $mpts$.

3) For a range of $mpts$ values, RNGs w.r.t. smaller values are contained in RNGs w.r.t. larger values of $mpts$, so that a *single* RNG is sufficient to compute the hierarchies for the whole range of $mpts$ values.

4) Information (related to "core-distances") that is needed in HDBSCAN* and that can be computed in a pre-processing step, allows us to formulate a highly efficient strategy for computing the single RNG, suitable for a whole range of $mpts$ values.

These results allow us to replace the (virtual) complete graph of the data, on which HDBSCAN* is based, with a single, pre-computed RNG that contains all the edges needed to compute the hierarchies for every value of $mpts \in [1, k_{max}]$. Moreover, this RNG has typically much fewer edges than the complete graph so its initial construction cost is more than outweighed by the reduction in edge weight computations.

The remainder of this paper is organized as follows. Section II discusses related work. Section III covers basic concepts and techniques used in this paper. Section IV presents our proposal and proves its correctness. Section V shows and discusses the results of our experimental evaluation. Section VI addresses the conclusions and some directions for future work.

II. RELATED WORK

To the best of our knowledge, there is no previous study of computing multiple clustering hierarchies efficiently. There has been work on automatic parameter selection strategies for density-based clustering, *e.g.*, [8], [17], [22], which are loosely related to the issue illustrated in Figure 1. However, those proposals are unsuitable to be used with HDBSCAN*, since they were developed for non-hierarchical clustering algorithms. In addition, they rely on assumptions that are often not satisfied in practice and there is not enough evidence to support their claims about parameter optimality.

If we denote the HDBSCAN*'s (virtual) complete graph for a given $mpts$ by G_{mpts}, a line of work related to our goal of reducing the cost for computing an MST for each G_{mpts},

are the works regarding (1) dynamically updating graphs, specifically MSTs, and (2) neighborhood graphs that could potentially replace HDBSCAN*'s (virtual) complete graph.

For instance, the works of [7], [13], [15], studied the problem of maintaining dynamic MSTs. However, these approaches more suitable when the changes in the underlying graph take place sequentially, that is, considering each operation (*e.g.*, edge updates) individually. When it comes to major changes taking place globally and simultaneously across the entire graph, as opposed to a few localized changes, a sequence of applications of these techniques tends to be computationally very costly, possibly even more costly than the construction of the entire MST from scratch. This is the case for G_{mpts}, which is a complete graph whose majority of edges will likely change as a result of a change in the $mpts$ value.

The works on neighborhood graphs that are most related to our proposal aim at speeding up the secial case of computing a *Euclidean* Minimum Spanning Tree (EMST), by first computing a spanning subgraph that is guaranteed to contain all the EMST edges. One of these strategies uses a Delaunay Triangulation [9] of the complete Euclidean graph G, since it has been shown that the EMST is contained in the Delaunay Triangulation of G [23]. Other spanning subgraphs of the complete graph G that contain the EMST are the Gabriel Graph [11], [20] and the Relative Neighborhood Graph (RNG) [23]. Unfortunately, these results are not simply applicable to our problem because G_{mpts} lies in a transformed space of the data that depends on $mpts$ ($G_{mpts} \neq G$), and it is one of the main contributions of this paper to formally show how to adapt an RNG so that it can be use by HDBSCAN* as a suitable replacement for G_{mpts} for different $mpts$.

III. BACKGROUND

A. HDBSCAN*

HDBSCAN* is a hierarchical, density-based clustering algorithm that improves on previous density-based algorithms [5]. Its main output is a cluster hierarchy that describes the nested structure of density-based clusters in a dataset with respect to a single parameter, $mpts$, which can be seen as a smoothing factor that can affect how and if certain clusters are represented in the hierarchy. A specific level at some "height" ε in this hierarchy represents a density level, specified by ε and $mpts$, in terms of density-based clusters and noise, defined as

follows: i) a point is either a *core point* w.r.t. ε and $mpts$ *iff* it has at least $mpts$ many points in its ε-neighborhood, or a *noise point* otherwise; ii) two core points are (directly) ε-*reachable* w.r.t. $mpts$ if they are within each other's ε-neighborhood; iii) two core points are *density-connected* w.r.t. ε and $mpts$ if they are directly or transitively ε-reachable w.r.t. $mpts$; and iv) a *cluster* w.r.t. ε and $mpts$ is a (non-empty) maximal subset of density connected points w.r.t. ε and $mpts$. To determine the *nested* structure of density-based clusters in a dataset $\mathbf{X}$, w.r.t. $mpts$, one needs to know (i) for each point $p \in \mathbf{X}$: the smallest value of ε such that p is a core point w.r.t. ε and $mpts$, called p's "core-distance" w.r.t. $mpts$; and (ii) for each value of ε: the clusters and the noise w.r.t. ε and $mpts$. The latter information can be derived conceptually from a complete, edge-weighted graph where nodes represent the points in $\mathbf{X}$, and the *edge weight* of an edge between two points p and q — called the "mutual reachability distance" (w.r.t. $mpts$) between p and q — is the smallest value of ε such that p and q are (directly) ε-reachable w.r.t. $mpts$. This graph is called the "Mutual Reachability Graph", G_{mpts}, which forms the conceptual basis of HDBSCAN*, and which we will discuss in more technical detail in the following subsection. For a specific density level (ε and $mpts$), removing all edges from G_{mpts} with weights greater than ε reveals the maximal, connected components, i.e., clusters, of that density level. The density-based clustering hierarchy can thus be compactly represented by (and more easily be extracted from) a Minimum Spanning Tree (MST) of G_{mpts}.

The HDBSCAN* hierarchy w.r.t. $mpts$ for a dataset $\mathbf{X}$ is computed in the following way: First, the core distances of all points in $\mathbf{X}$ w.r.t. $mpts$ are computed. Then, an MST of G_{mpts} is dynamically computed (without materializing G_{mpts}). From this MST, the *complete* density-based cluster hierarchy w.r.t. $mpts$ is then extracted, by removing edges from the MST in descending order of edge weight, and (re-)labeling the connected components and noise at the resulting "next" level.

B. Mutual Reachability Graphs

The G_{mpts} is a complete, edge-weighted graph that represents the mutual reachability relationship between any two points in a dataset $\mathbf{X}$. Each point in $\mathbf{X}$ corresponds to a vertex, and between each pair of points p and q, there is an edge whose weight is defined as the Mutual Reachability Distance between p and q w.r.t. $mpts$, mrd_{mpts} [19]:

$$mrd_{mpts}(p,q) = max\{c_{mpts}(p), c_{mpts}(q), d(p,q)\} \quad (1)$$

where $d(\cdot,\cdot)$ represents the underlying distance function (typically Euclidean distance), and $c_{mpts}(p)$ represents the core distance of p, which is formally the distance from p to its $mpts$ nearest neighbor, $mpts$-NN(p):

$$c_{mpts}(p) = d(p, mpts\text{-NN}(p)) \quad (2)$$

In this work, we assume that the underlying distance $d(\cdot,\cdot)$ satisfies Symmetry and Triangle Inequality, and, without loss of generality, we use Euclidean Distance in our examples.

Intuitively, an edge weight in G_{mpts} corresponds to the minimum radius ε at which the corresponding endpoints are directly ε-reachable w.r.t. $mpts$, *i.e.*, the smallest distance at which both points are in each other's ε-neighborhood, and both ε-neighborhoods contain at least $mpts$ points.

The Mutual Reachability Graph has the following important characteristics related to mrd_{mpts} and to how these edge weights change when changing the value of $mpts$: 1) Increasing the value of $mpts$ leads, in general, to higher values of c_{mpts}, since c_{mpts} is the $mpts$-th nearest neighbor distance; 2) When increasing the value of c_{mpts}, more edges will have the same edge weight, since a point p with a high c_{mpts} determines the weight of all edges between p and its $mpts$-nearest neighbors that have a smaller c_{mpts} than p (given that mrd_{mpts} is defined by a max function); 3) When decreasing the value of $mpts$, edge weights can either decrease or remain the same, but never increase.

The authors of HDBSCAN* [5], [6] deem G_{mpts} a conceptual graph as it does not need to be explicitly stored; edge weights can be computed on demand, when needed.

IV. APPROACH

At the core of HDBSCAN* is the computation of an MST from the G_{mpts} of a dataset. The time needed to compute an MST depends on the number of edges of the input graph, which in case of G_{mpts} is a complete graph. Even if G_{mpts} is not materialized, $O(n^2)$ edge weights have to be processed for a dataset with n points.

When HDBSCAN* has to be run for a range, $k_1, \ldots, k_{max}$, of $mpts$ values, many MSTs have to be computed for different G_{mpts} graphs, one for each value of $mpts \in \{k_1, \ldots, k_{max}\}$. Conceptually, we can think of each G_{mpts} being obtained by taking the complete, unweighted graph G of the dataset, and then incorporate into it appropriate edge weights, which means that edge weights of G_{mpts} have to be re-computed for each $mpts \in \{k_1, \ldots, k_{max}\}$ before an MST is constructed.

One way to speed up the execution time of HDBSCAN* over all values of $mpts \in \{k_1, \ldots, k_{max}\}$, even with a naive approach of re-running HDBSCAN* for each $mpts$ value, is to execute k-Nearest-Neigbor (k-NN) queries for each point only once, using the largest value k_{max} in the range. When computing the core distance of a point p w.r.t. $mpts = k_{max}$ using a k_{max}-NN query, the information about *all smaller* core distances of p (*i.e.*, w.r.t. $mpts = k_j$, where $j \leq max$), is readily available as part of the k_{max}-NN query computation. Hence, the core distances for all values of $mpts \in \{k_1, \ldots, k_{max}\}$ can be pre-computed and stored so that the re-computation of edge weights (reachability distances) for the different G_{mpts} graphs does not require additional k-NN-queries. However, even with pre-computed core distances, a major factor determining the total runtime of HDBSCAN*, over all values of $mpts \in \{k_1, \ldots, k_{max}\}$, is the large number of edges that have to be processed in the MST constructions for each value of $mpts$.

To reduce the number of edges that have to be processed, we can ask the questions: is it possible to construct a single

graph that is significantly smaller than a complete graph, and that contains all the edges needed to compute the MST of G_{mpts} for all $mpts \in \{k_1, \ldots, k_{max}\}$? If the answer is *yes*, we can use this graph instead of the complete graph in HDBSCAN*, without changing the correctness of the result: we can just re-compute its edge weights instead of the edge weights of the complete graph, for each value of $mpts \in \{k_1, \ldots, k_{max}\}$, and compute the MST of *this* edge-weighted graph. In the following, we will formally prove that one of the known graphs can be adapted so that it can be used in our approach to running HDBSCAN* for each value of $mpts \in \{k_1, \ldots, k_{max}\}$. How much speed-up can be achieved in this manner depends, however, not only on the reduction in number of edges from the complete graph, but also on the added computational cost for constructing this graph.

A. Results from Computational Geometry

Consider first the special case of $mpts = 1$, where all core distances are equal to zero, and thus the mutual reachability distance mrd_{mpts} reduces to the underlying distance function. With Euclidean distance, what HDBSCAN* has to compute then is the Euclidean Minimum Spanning Tree (EMST) of a dataset $\mathbf{X}$, i.e., the MST of a complete graph of $\mathbf{X}$ (containing an edge between every pair of points/vertexes) with Euclidean distance between points as edge weights.

For the EMST, there are known results from computational geometry that relate the EMST to some of the so-called *proximity graphs*, in which two points are connected by an edge whenever a certain spatial constraint is satisfied. The most popular ones are the Delaunay Triangulation (DT), the Gabriel Graph (GG) and the Relative Neighborhood Graph (RNG), for which it has been shown that [23]:

$$EMST \subseteq RNG \subseteq GG \subseteq DT \qquad (3)$$

The RNG and GG are special cases of a family of graphs called β-skeletons [18], which can range from the complete graph to the empty graph, when β goes from 0 to ∞. A value of $\beta = 1$ results in the GG and $\beta = 2$ results in the RNG.

Given this result, the RNG, or possibly a β-skeleton with even fewer edges, may be a good replacement for a complete graph, if we can answer the following questions positively:

1) Can we determine the smallest β-skeleton, in terms of number of edges, that contains the EMST as a subgraph?
2) Can the results we have for Euclidean distance be generalized to other reachability distances w.r.t. $mpts > 1$?
3) Is there a single β-skeleton that contains all the edges needed to compute an MST of G_{mpts} for each value of $mpts$ in a range of values $k_1, \ldots, k_{max}$?
4) Does the reduction in the number of edges justify the additional computational cost for constructing and materializing a β-skeleton for our task?

We will answer these questions in the following subsections.

B. The Smallest β-Skeleton Containing the EMST

The family of β-skeletons for a set of d-dimensional points is defined in the following way. For a given β, an edge exists

(a) $\beta = 2$ (b) $\beta > 2$

Fig. 2: β-skeletons
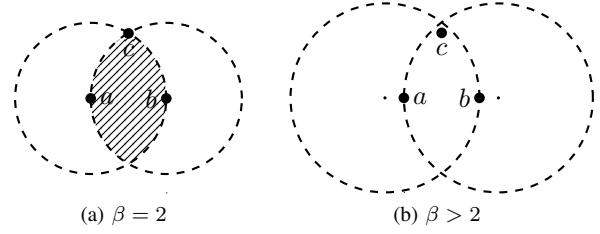
between two points a and b if the intersection of the two balls centered at $(\beta/2)a + (1 - \beta/2)b$ and $(1 - \beta/2)a + (\beta/2)b$, both with radius $\beta d(a,b)/2$, is empty. For instance, when $\beta = 2$ (the case of an RNG), the centers of the two balls coincide with the points a and b, and their radius is equal to $d(a,b)$, as illustrated in Figure 2a. The highlighted region, called $lune(a,b)$, must be empty for a and b to be connected via an edge. For $\beta = 2$, one can equivalently say that an edge exists between a and b if

$$d(a,b) \leq max\{d(a,c), d(b,c)\}, \forall c \neq a, b \qquad (4)$$

The RNG is guaranteed to contain the EMST, which has been shown in [23]. The essence of the proof can be demonstrated considering a configuration of three points a, b, c, such that $lune(a,b)$ contains c, as shown in Figure 3a. The edges (a,b), (a,c) and (b,c) cannot all be part of an EMST, as they form a cycle. Since (a,b) is the largest of these edges, (a,b) cannot be part of the EMST. Thus, a necessary (yet not sufficient) condition for an edge (a,b) to be in an EMST is that all other points must lie outside $lune(a,b)$. In other words, we can remove all edges $(a,b) \in E$ from the complete graph G whose points a and b have a non-empty lune, and be sure that the resulting graph $(V, E \setminus \{(a,b) : lune(a,b) \neq \emptyset\}) = RNG$ contains the EMST. Here, we prove by counter example that the RNG is actually the smallest β-skeleton graph (i.e., there is no $\beta > 2$) with that property. Consider a dataset with three points a, b and c, located at equal distance from each other, as illustrated in Figure 2: When $\beta = 2$ (Figure 2a), according to Inequality (4), there is an edge between every pair of points in the 2-skeleton of this dataset. For any $\beta > 2$ (Figure 2b), however, the radius of the balls that define $lune(a,b)$ is increased by a factor of $(\beta - 2)/2$, and the centers of the balls are "pulled apart" accordingly, so that c (equidistant from a and b) must now be inside $lune(a,b)$. Thus, a and b are (by definition of β-skeleton) no longer connected by an edge. Analogously, there is no edge between the other pairs of points for $\beta > 2$, resulting in an empty β-skeleton that obviously cannot contain the EMST (i.e., $EMST \nsubseteq \beta$-skeleton $\forall \beta > 2$). From this result and from the known result in Expression (3), the RNG ($\beta = 2$) is thus the smallest β-skeleton graph that contains the EMST and, for this reason, we choose it as the basis for further analysis.

C. The RNG w.r.t. Mutual Reachability Distance

In this section, we prove that the results for RNGs in Euclidean space can be extended to the space of mutual reachability distances.

Notation: (1) Let $G = (V, E)$ denote the undirected, unweighted complete graph corresponding to a dataset, *i.e.*, the set of vertexes V represents the data points, and the set of edges $E \subset V \times V$ represents all pairs of vertexes/points. (2) Let $G_i = (V, E, mrd_i)$ be the mutual reachability graph G_{mpts} for $mpts = i$, *i.e.*, the weighted, complete graph for the dataset with edge weights equal to mrd_i, the mutual reachability distance w.r.t. $mpts = i$.

We can define a relative neighborhood graph w.r.t. the mutual reachability distance mrd_i, RNG^i, as follows:

Definition 1: $RNG^i = (V, E')$ where $E' \subseteq E$ and there is an edge $(a, b) \in E'$ if and only if:

$$mrd_i(a, b) \leq max\{mrd_i(a, c), mrd_i(b, c)\}, \forall c \neq a, b;$$

and when there is an edge $(a, b) \in E'$, we say that a and b are relative neighbors w.r.t mrd_i. The unweighted graph RNG^i can be extended with edge weights defined by a distance function mrd_j, which results in the edge weighed graph RNG^i_j, where the weight of an edge connecting two points p and q is equal to $mrd_j(p, q)$.

We can prove that the RNG^i_i contains the MST of G_i, and thus we can replace G_i with RNG^i_i when running HDBSCAN* for $mpts = i$.

Theorem 1: $MST(G_i) \subseteq RNG^i_i$

Proof 1: The argument for why $EMST \subseteq RNG$, which has been shown in [23], relies in essence only on the fact that the Euclidean Distance is symmetric and satisfies the triangle inequality; it is, in fact valid for any distance function with these properties, which are needed to guarantee that (a, b) is in fact the largest edge in configurations like the one shown in Figure 3a. Consequently, we only need to show that mrd_i satisfies symmetry and triangle inequality.

For symmetry, we can easily see from the definition of mrd_{mpts} in Equation (1) that $mrd_i(a, b) = mrd_i(b, a)$ (given that the underlying distance d is symmetric by assumption).

For the triangle inequality, we have to show that for all a, b, c in a dataset X:

$$mrd_i(a, c) \leq mrd_i(a, b) + mrd_i(b, c) \qquad (5)$$

By assumption (Section III), the underling distance d in definition of mrd_i satisfies the triangle inequality, *i.e.*:

$$d(a, c) \leq d(a, b) + d(b, c) \qquad (6)$$

There are three cases according to the definition of $mrd_i(a, c)$, in all of which the triangle inequality must hold:

1) $mrd_i(a, c) = c_i(a)$. The max function in the definition of mrd_i implies $c_i(a) \leq mrd_i(a, b)$. Hence, it follows that $mrd_i(a, c) = c_i(a) \leq mrd_i(a, b) \leq mrd_i(a, b) + mrd_i(b, c)$.

2) $mrd_i(a, c) = c_i(c)$. Analogous to case 1).

3) $mrd_i(a, c) = d(a, c)$. Since for any x, y it holds that $x \leq max(x, y)$, we can replace the terms on the right side
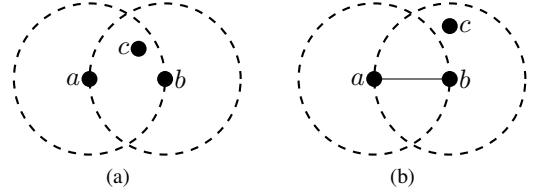

Fig. 3: Illustration for proofs of Theorem 1 and 2

of Inequality (6) with max functions to obtain, $d(a, c) \leq max\{d(a, b), c_i(a), c_i(b)\} + max\{d(b, c), c_i(b), c_i(c)\} = mrd_i(a, b) + mrd_i(b, c)$, and hence, also in this case: $mrd_i(a, c) = d(a, c) \leq mrd_i(a, b) + mrd_i(b, c)$.

Since mrd_i satisfies symmetry and triangle inequality, it follows from [23] that RNG^i_i contains the MST of G_i.

D. One RNG To Rule Them All

We have established that we can use RNG^i_i as a substitute for G_i in HDBSCAN*. We will now show that all MSTs for HDBSCAN* hierarchies w.r.t. $mpts \in \{k_1, \ldots, k_{max}\}$ can be obtained from the single graph $RNG^{k_{max}}$. For this we only need to show that $RNG^i \subseteq RNG^{k_{max}}$, for all $i < k_{max}$. If this property holds, we can use the single graph $RNG^{k_{max}}$ to compute the MST of any G_i by first equipping $RNG^{k_{max}}$ with edge weights mrd_i, and then computing the MST of this edge-weighted graph $RNG^{k_{max}}_i$. Compared to the naive approach that uses the complete graph G in this manner, we should be able to speed up the MST computations by using a graph that has typically much fewer edges.

Theorem 2: $RNG^i \subseteq RNG^{k_{max}}, \forall i < k_{max}$.

Proof 2: To prove this by contradiction, assume that there is a $j < k_{max}$ for which this property does not hold, *i.e.*, $RNG^j \nsubseteq RNG^{k_{max}}$. Then, there must be at least one edge (a, b) that belongs to RNG^j but does not belong to $RNG^{k_{max}}$. According to the condition that defines relative neighborhood graphs, this means that there is a point c, such that for distance $mrd_{k_{max}}$, $c \in lune(a, b)$, and for distance mrd_j, $c \notin lune(a, b)$, as illustrated in Figure 3.

For $RNG^{k_{max}}$ (Figure 3a) this means that the following inequalities must *both* be satisfied so that $c \in lune(a, b)$.

$$mrd_{k_{max}}(a, b) > mrd_{k_{max}}(a, c) \qquad (7)$$
$$mrd_{k_{max}}(a, b) > mrd_{k_{max}}(b, c) \qquad (8)$$

For RNG^j (Figure 3b) this means that *at least one* of the following inequalities must be satisfied so that $c \notin lune(a, b)$.

$$mrd_j(a, b) \leq mrd_j(a, c) \qquad (9)$$
$$mrd_j(a, b) \leq mrd_j(b, c) \qquad (10)$$

Using the definition of $mrd_{k_{max}}$, we can rewrite Inequalities (7) and (8) as follows:

$$max\{c_{k_{max}}(a), c_{k_{max}}(b), d(a, b)\}$$
$$> \qquad (11)$$
$$max\{c_{k_{max}}(a), c_{k_{max}}(c), d(a, c)\}$$

$$max\{c_{k_{max}}(a), c_{k_{max}}(b), d(a,b)\}$$
$$> \tag{12}$$
$$max\{c_{k_{max}}(b), c_{k_{max}}(c), d(b,c)\}$$

There are theoretically three cases, $c_{k_{max}}(a)$, $c_{k_{max}}(b)$, and $d(a,b)$, that the max function on the left-hand side of the Inequalities (11) and (12) can evaluate to. However, for both inequalities to be true simultaneously, only $d(a,b)$ is possible:

1) Case $max\{c_{k_{max}}(a), c_{k_{max}}(b), d(a,b)\} = c_{k_{max}}(a)$.
In this case, we get from Inequality (11) the following:

$$c_{k_{max}}(a) > max\{c_{k_{max}}(a), c_{k_{max}}(c), d(a,c)\}$$

But since $max(c_{k_{max}}(a), \dots) \geq c_{k_{max}}(a)$, it follows that $c_{k_{max}}(a) > c_{k_{max}}(a)$, a contradiction!

2) Case $max\{c_{k_{max}}(a), c_{k_{max}}(b), d(a,b)\} = c_{k_{max}}(b)$.
In this case, analogously to the previous case, if follows from Inequality (12) that $c_{k_{max}}(b) > c_{k_{max}}(b)$, a contradiction!

3) Case $max\{c_{k_{max}}(a), c_{k_{max}}(b), d(a,b)\} = d(a,b)$.
In this case there is no contradiction and, therefore, it is the only option to satisfy both (11) and (12) simultaneously.

Having established that the left-hand side of Inequalities (11) and (12) must be equal to $d(a,b)$, we can infer that all the following inequalities must hold.

$$d(a,b) > c_{k_{max}}(a) \tag{13}$$
$$d(a,b) > c_{k_{max}}(b) \tag{14}$$
$$d(a,b) > c_{k_{max}}(c) \tag{15}$$
$$d(a,b) > d(a,c) \tag{16}$$
$$d(a,b) > d(b,c) \tag{17}$$

Let us now turn to the Inequalities (9) and (10) of which at least one must also hold, under our assumption that $c \notin lune(a,b)$ for distance mrd_j. We can rewrite (9), using the definition of mrd_j as follows:

$$max\{c_j(a), c_j(c), d(a,c)\}$$
$$\geq \tag{18}$$
$$max\{c_j(a), c_j(b), d(a,b)\}$$

There are again three possible cases, $c_j(a), c_j(c), d(a,c)$, that the max function on the left-hand side of Inequality (18) can evaluate to, and we show that each one leads to a contradiction to what we already know about a, b, and c:

1) $max\{c_j(a), c_j(c), d(a,c)\} = c_j(a)$.
In this case, Inequality (18) yields the following.

$$c_j(a) \geq d(a,b) \tag{19}$$

Since core distances c_{mpts} can only increase when $mpts$ increases, we have $c_{k_{max}}(a) \geq c_j(a)$ and, accordingly, we obtain the following from Inequality (19).

$$c_{k_{max}}(a) \geq d(a,b) \tag{20}$$

This contradicts Inequality (13)!

2) $max\{c_j(a), c_j(c), d(a,c)\} = c_j(c)$.
Analogously to the previous case, from (18) we get (21), and

then from $c_{k_{max}}(c) \geq c_j(c)$ we get (22), which contradicts Inequality (15)!

$$c_j(c) \geq d(a,b) \tag{21}$$
$$c_{k_{max}}(c) \geq d(a,b) \tag{22}$$

3) $max\{c_j(a), c_j(c), d(a,c)\} = d(a,c)$.
In this case, we get from Inequality (18) that $d(a,c) \geq d(a,b)$, which is a contradiction to Inequality (16)!

This proves that Inequality (9) cannot hold under our assumption. We can prove analogously the same result for Inequality (10), which contradicts our assumption that there is a $j < k_{max}$ such that $RNG^j \nsubseteq RNG^{k_{max}}$. Hence $RNG^i \subseteq RNG^{k_{max}}$, $\forall i \leq k_{max}$.

When we combine the results of Theorems 1 and 2, we obtain the following corollary, which states that the $MST(G_i)$ for all $i < k_{max}$ is contained in $RNG^{k_{max}}$, and can thus be obtained by extending $RNG^{k_{max}}$ with edge weights mrd_i, and computing the MST of this graph $RNG_i^{k_{max}}$.

Corollary 1: $MST(G_i) \subseteq RNG_i^{k_{max}}$, $\forall i \leq k_{max}$.

Proof 3: $MST(G_i) \subseteq RNG_i^i$ (Theorem 1), and $RNG^i \subseteq RNG^{k_{max}}$ (Theorem 2). By extending both graphs from Theorem 2 with edge weights mrd_i, we obtain $RNG_i^i \subseteq RNG_i^{k_{max}}$. Hence, $MST(G_i) \subseteq RNG_i^{k_{max}}$.

E. RNG Computation

The performance gain when running HDBSCAN* w.r.t. all values of $mpts \in \{k_1, \dots, k_{max}\}$ by using $RNG^{k_{max}}$ instead of the complete graph G of a dataset relies on a number of factors: the complexity of the additional time to construct $RNG_i^{k_{max}}$ (recall that G does not have to be explicitly constructed), the number of edges in $RNG_i^{k_{max}}$ compared to G, and the number of hierarchies k_{max} to be computed.

The naive way to compute an RNG for a set of points **X** is to check for every pair of points $p, q \in \mathbf{X}$ and each point c, whether c is inside $lune(p,q)$. This algorithm runs in $O(n^3)$ time, which is inefficient for large datasets. More efficient strategies are surveyed in [16].

We adopt the approach in [1] —which has sub-quadratic expected time complexity under the assumption that points are in general position— with an adaptation of the definition of well-separated pairs proposed in [4]. This approach has three main steps.

In the first step, the entire dataset is decomposed recursively into smaller and smaller subsets (see [4] for details), so that all pairs of obtained subsets (A, B) are *well-separated*. The notion of well-separability requires the smallest possible distance between any point $a \in A$ to any point $b \in B$ to be larger than the largest possible distance between points within each of the two sets. For efficiency reasons one does not compute pairwise distances, but instead uses "safe" bounds that can be efficiently computed to determine well-separability of two sets. The distance is in our case the mutual reachability distance mrd_{mpts}, and the smallest possible mrd_{mpts} between two point sets A and B is, because of the max function in the definition of mrd_{mpts}, the shortest possible Euclidean distance between a point $a \in A$ and a point $b \in B$. This distance

$D(A, B)$ can be bounded, as in [4], by the distance between the smallest enclosing balls B_A and B_B around the minimum bounding hyper-rectangles enclosing A and B, respectively. Then, we can define that A and B are well-separated if:

$$D(A, B) \geq$$
$$s \cdot \max\{diameter(B_A), diameter(B_B), \max_{p \in A \cup B}(c_{mpts}(p))\}$$

$max\{diameter(B_A), diameter(B_B), \max_{p \in A \cup B}(c_{mpts}(p))\}$ represents a bound on the largest possible mutual reachability distance within the sets A and B. The separation factor $s > 0$ determines how far both sets have to be from each other to be considered *well-separated*. The larger the separation factor, the larger the number of generated pairs. For $0 < s < 1$, there is no guarantee that the resulting graph will contain the MST edges, and hence we adopt $s = 1$.

In the second step, all the well-separated pairs are connected with edges such that a supergraph of the RNG, which we will call RNG**, is obtained. For each pair (A, B), the points $a_i \in A$ and $b_j \in B$ are connected with an edge if they are Symmetric Bichromatic Closest Neighbors (SBCN), *i.e.*, if there is no other point in B that is closer to a_i than b_j and vice versa. For example, in Figure 4, the points a_3 and b_3 are SBCN and thus the edge (a_3, b_3) is part of the RNG**.

The third step of the RNG computation consists of filtering RNG** to remove edges that are not in the RNG. Although RNG** has typically far fewer edges than the complete graph G, a naive filtering approach, which checks for each edge (a, b) in RNG**whether each point c is in $lune(a, b)$, can be extremely time consuming for large datasets. Therefore, we propose an alternative strategy using information that is computed anyway for HDBSCAN*, which can make the overall filtering process more efficient. It is based on the intuition that points closer to a or b are more likely in $lune(a, b)$ than points that are farther away. For computing multiple HDBSCAN* hierarchies, we initially compute all the needed core distances by performing a single k_{max}-nearest neighbor query for each point, which means that we do find the k_{max} closest points to each point. To support our pruning strategy, we only have to store in addition to the c_i values also the actual $mpts$-nearest neighbors. Using this information, for each edge (a, b) with weight w, we first check if any of the $mpts$-nearest neighbor of a and b is inside $lune(a, b)$. As soon as we find one that is inside, we can safely remove the edge without further checking. If none of those neighbors is inside $lune(a, b)$, we check if w is equal to the core-distance of a or b. If that is the case (say for a), we know that no other point can be in $lune(a, b)$ (since $lune(a, b)$ is a subset of the ball around a with radius w and we have checked all points inside this ball); hence we know without further checking that the edge is in the RNG. We can choose to perform only these $2 \times k_{max}$ checks per edge to obtain a graph, which we call RNG*, that is smaller than RNG** but may contain more edges than the RNG. To obtain the exact RNG, we search the entire dataset whenever we cannot exclude or include an edge
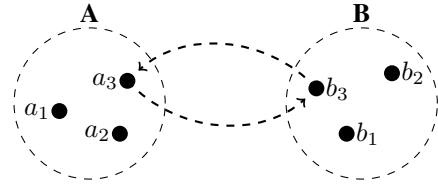

Fig. 4: Symmetric Bichromatic Closest Neighbor (SBCN)

based on the $2 \times k_{max}$ tests, to determine whether or not there is a point in $lune(a, b)$.

Algorithm 1

Input: X: dataset; n: $|X|$; $[k_1, \ldots, k_{max}]$: $mpts$ range; T: graph to be computed (RNG, RNG, RNG**);

1: **for** $i \in \{1, ..., n\}$ **do**
2:     **for** $j \in \{k_1, \ldots, k_{max}\}$ **do**
3:         $M[i][j] \leftarrow (j^{th}\text{-NN}(i), c_j(i))$;
4:
5: $wspd \leftarrow WSPD(X, M)$;
6:
7: **for** $(A, B) \in wspd$ **do**
8:     $RNG^{k_{max}} \leftarrow RNG^{k_{max}} \cup SBCN(A, B)$;
9:
10: $remove \leftarrow$ False;
11:
12: **if** $T \neq$ RNG** **then**
13:     **for** $(a, b) \in RNG^{k_{max}}$ **do**
14:         **for** $x \in M[a] \cup M[b]$ **do**
15:             **if** $x \in lune(a, b)$ **then**
16:                 $remove \leftarrow$ True;
17:                 **break;**
18:         **if** $\neg \, remove$ **then**
19:             **if** $mrd_{k_{max}}(a, b) = max\{c_{k_{max}}(a), c_{k_{max}}(b)\}$ **then**
20:                 $remove \leftarrow$ False;
21:                 **continue;**
22:         **if** $\neg \, remove$ and $T =$ RNG **then**
23:             **for** $x \in X$ **do**
24:                 **if** $x \in lune(a, b)$ **then**
25:                     $remove \leftarrow$ True;
26:                     **break;**
27:         **if** $remove$ **then**
28:             $RNG^{k_{max}} \leftarrow RNG^{k_{max}} \setminus (a, b)$;
29:             $remove \leftarrow$ False;
30:
31: **for** $mpts \in \{k_1, \ldots, k_{max}\}$ **do**
32:     $MST_{mpts} \leftarrow MST(RNG^{k_{max}}_{mpts})$;
33:     $compute\text{-}hierarchy(MST_{mpts})$;

The pseudo-code for the overall strategy is shown in Algorithm 1. It takes as input a dataset **X** with n points, a range of $mpts$ values, $[k_1, \ldots, k_{max}]$, and the type T of the RNG to be computed. All the core-distances for each point $x \in \mathbf{X}$ and its corresponding k-NN neighbors, for $k \in \{k_1, \ldots, k_{max}\}$, are computed in Lines 1-3. It is important to emphasize that a single k_{max}-NN query is performed for each $x \in \mathbf{X}$. The statement in Line 3 illustrates the format of the entries of the matrix M. Next, the Well-Separated Pairs Decomposition (WSPD) is performed in Line 5. In Lines 7-8, the RNG** is constructed by adding one edge for each of the Symmetric

Bichromatic Closest Neighbors (SBCN) between the pairs $(A, B) \in wspd$. The edge filtering occurs between Lines 13-29. In case the RNG** is chosen, the filtering process is completely skipped (Line 12). Otherwise (both RNG* and RNG), the filter steps based on the k_{max}-nearest neighbors are performed. The last filter, based on the sequential scan of the dataset (Lines 23-26), is only performed when the RNG is to be computed. At the end (Lines 31-33), the MSTs and hierarchies are computed for all the values of $mpts \leq k_{max}$, using the computed RNG.

Note that, if one has to compute just a single MST from G, even though this operation is quadratic in the number of points since it depends on the number of edges in G, it may not pay off to first construct $RNG^{k_{max}}$. However, as the number of hierarchies that have to be computed increases, the initial overhead of constructing $RNG^{k_{max}}$ can substantially speed up the overall time to complete the k_{max} MSTs, if the number of edges in $RNG^{k_{max}}$ is much smaller than in G.

V. Experiments

We conducted experiments to evaluate the efficiency of the proposed method with respect to changes in size and dimensionality of the dataset, and, most importantly, with respect to the number of hierarchies to be computed. We also show the RNG, RNG*, and RNG** sizes in comparison to the size of the G_{mpts}, since the difference in the number of edges is the source of our performance gain.

To the best of our knowledge, there is no other strategy in the literature that aims at computing multiple hierarchies efficiently. Thus, we compare our strategy to a straightforward baseline that runs HDBSCAN* multiple times, one for each $mpts$ value in the given range, but with the optimization of pre-computing the core distances for all points, in the same way we do in our approach (see Section IV), so that kNN queries are only executed once and not for each value of $mpts$.

To study the computational trade-offs of the different edge filtering strategies described in Subsection IV-E, we show results for three variants: RNG**-HDBSCAN*, which just uses the RNG** without any additional filtering; RNG*-HDBSCAN*, which applies only the filtering based on k_{max} nearest neighbors; and RNG-HDBSCAN*, which applies the complete filtering to obtain the exact RNG.

All methods have been implemented on top of the original HDBSCAN* code, provided by the authors of [6], in Java. The core-distances are computed with the aid of a Kd-Tree index structure, adapted from [24]. The experiments were performed in a virtual machine with 64GB RAM, running Ubuntu. For runtime experiments, we measure the total running time to compute core-distances and MSTs, and report the average runtime over 5 experiments.

The datasets were obtained using the generator proposed in [12], varying the number of dimensions from 2 to 128, the number of points from 16k to 1M, and the value of k_{max} from 2 to 128. Table I shows these values and indicates in bold the default value for each variable when other variables are varied.

TABLE I: Experimental Setup

Variables	Values
#points	16k, 32k, 64k, **128k**, 256k, 512k, 1M
#dimensions	2, 4, 8, **16**, 32, 64, 128
k_{max}	2, 4, 8, **16**, 32, 64, 128

A. Effect of Dataset Size

Figure 5a shows the total runtime as a function of the dataset size with default values for the remaining variables (i.e., computing 16 MSTs in 16-dimensional datasets). As expected, the runtime tends to increase as the number of points increases for all methods. For datasets up to 64k points, all strategies have similar performances, but for larger datasets the difference between our approaches and the baseline increases significantly as the number of points increases. For 128k points, the baseline strategy already takes approximately twice as much time as our approaches. For 1024k points, we actually interrupted each run of the baseline before it finished.

Figure 6a shows the number of edges in G_{mpts}, RNG**, RNG*, and RNG, as a function of the dataset size. As expected, the number of edges increases with the number of points. However, the RNGs are significantly smaller than the complete graph for all dataset sizes. In fact, even for the largest dataset, the sizes of the RNG* and RNG are smaller than the size of the G_{mpts} for the smallest dataset.

When comparing RNG and RNG**, the time spent filtering to obtain the exact RNG is compensated by a smaller graph size, which in turn results in faster MST computations. This explains why both RNG and RNG** exhibit similar running times in Figure 5a, despite the differences in their sizes. Only when the partial fast filter based on k-nearest neighbors is applied to obtain RNG*, the total runtime is faster. This is because the filter is effective in producing a graph that is almost as small as the exact RNG, yet in less time.

B. Effect of Dimensionality

Figure 5b shows the effect of dataset dimensionality on the runtimes. As expected, all approaches are affected by increasing dimensionality, since most of the underlying techniques for clustering, kNN queries, and RNG computation are bound to eventually become less effective as dimensionality increases. This is due to a number of effects that are generally referred to as "curse of dimensionality." However, since our datasets do contain cluster structures, these effects are not critically severe even in 128 dimensions.

We can observe that all RNG-based strategies perform better than the baseline in all datasets, but as dimensionality increases, the difference between the unfiltered RNG (RNG**) and the filtered versions (RNG* and RNG) increases. This can be explained by looking at the number of graph edges, as shown in Figure 6b. The size of the exact RNG is barely affected by an increase of dimensionality in these datasets, while the unfiltered RNG** exhibits a pronounced growth in
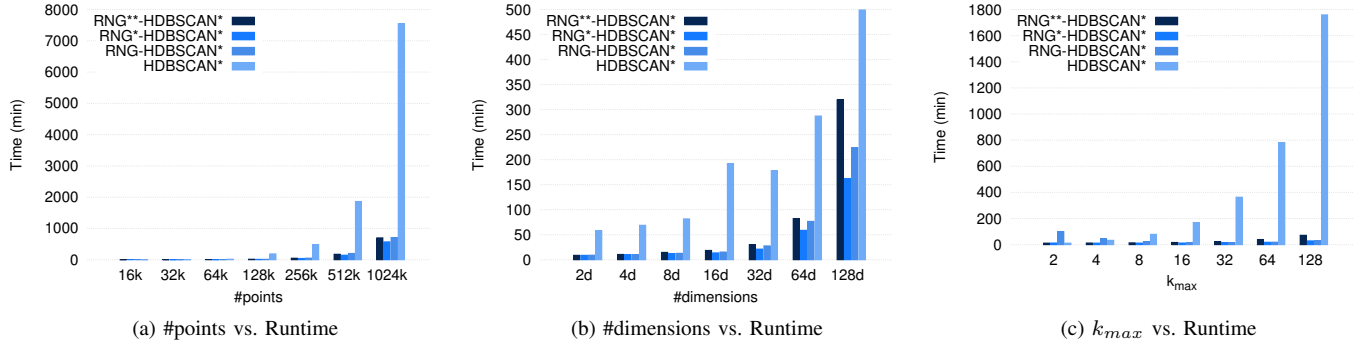
(a) #points vs. Runtime   (b) #dimensions vs. Runtime   (c) k_{max} vs. Runtime

Fig. 5: Runtime as a function of the dataset size, dataset dimensionality, and k_{max}. (Note that the x-axis is in log scale.)

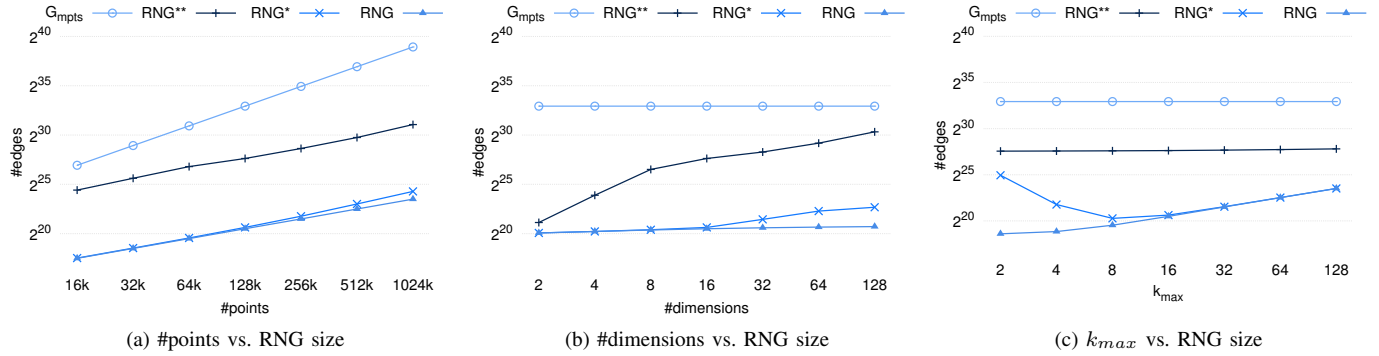(a) #points vs. RNG size   (b) #dimensions vs. RNG size   (c) k_{max} vs. RNG size

Fig. 6: RNG size as a function of the dataset size, dataset dimensionality, and k_{max}. (Note that both axes are in log scale.)
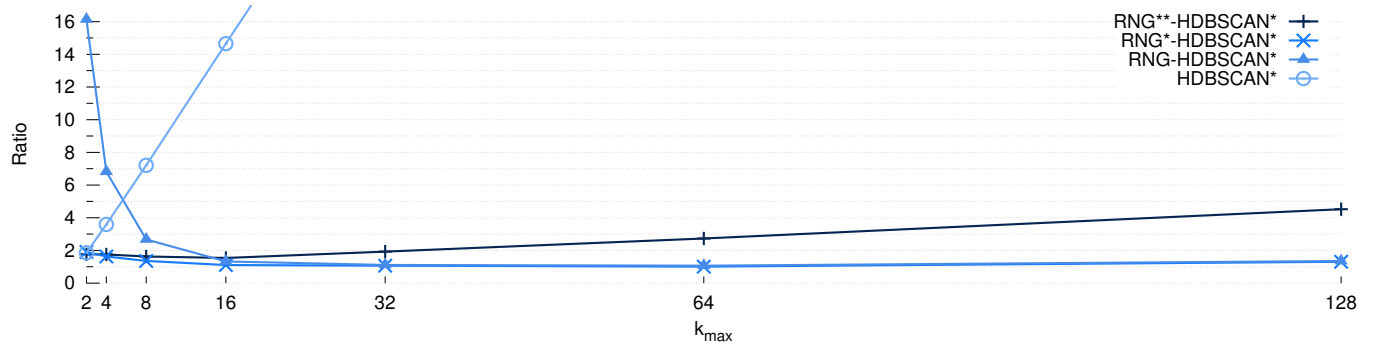

Fig. 7: Ratio: runtime to compute k_{max} MSTs/hierarchies divided by the runtime to compute a single MST/hierarchy.

the number of edges, which approaches the complete graph G_{mpts}. This shows that the generation of well-separated pairs is very sensitive to dimensionality, becoming less effective in implicitly excluding edges that cannot be in an RNG. On the other hand, the exact relative neighborhood graph still has significantly fewer edges than a complete graph in these scenarios —although, theoretically, it also must eventually approach the complete graph [3], [16].

Notably, the number of edges for RNG* increases only slightly as the dimensionality increases, which shows that the pruning strategy using only the pre-computed k-nearest

neighbors (16, as $k_{max} = 16$ in this experiment) stays quite effective, even in the 128-dimensional datasets, resulting in the best runtime performance overall.

C. Effect of Upper Limit k_{max}

Figure 5c and Table II show the runtimes w.r.t. k_{max}. The runtime of all our methods is very low compared to the baseline, for which runtime increases linearly, as expected. The runtime of HDBSCAN*-RNG** increases very slightly with k_{max} as also the number of edges increases slightly, but stays significantly below the number of edges in G_{mpts}, as shown in Figure 6c.

TABLE II: k_{max} vs. Runtime (min.)

k_{max}	HDBSCAN*	RNG**-HDBSCAN*	RNG*-HDBSCAN*	RNG-HDBSCAN*
2	**12**	**12**	**12**	99
4	33	**12**	**12**	45
8	79	14	**12**	22
16	169	17	**13**	15
32	363	23	**14**	15
64	781	40	**18**	19
128	1759	72	**29**	30

RNG-HDBSCAN* shows a slightly higher runtime for $mpts = 2$, which then decreases for $mpts = 4$ and $mpts = 8$, after which it stays almost constant and becomes almost indistinguishable in performance to RNG*-HDBSCAN*. RNG*-HDBSCAN*, which only uses the k_{max}-nearest neighbors of objects for pruning RNG**, shows the most stable runtime behavior; its increase in runtime as k_{max} increases is almost unnoticeable. For the largest value of k_{max}, its difference in runtime to the baseline method corresponds to a speedup of about 60 times. The runtime behavior of RNG and RNG* can be explained by the number of edges in RNG and RNG*, shown in Figure 6c. For $mpts = 2$, the number of edges in RNG* is much larger than in RNG (while still being smaller than in RNG**). The reason is that the the filtering strategy based on the k_{max}-NN is not yet very effective when only the two nearest neighbors are considered. In this case, for all the edges that are removed from RNG* to obtain RNG, a sequential scan has to be performed, which is overall more costly in terms of runtime than the gain in runtime for computing the MST of RNG with fewer edges. These results also show that (1) computing MSTs is very fast, compared to the rest of the computation, if the underlying graphs are already relatively small compared to the complete graph, and (2) our pruning heuristic based on k_{max}-NNs becomes more effective as k_{max} increases, leading to an almost indistinguishable performance between RNG and RNG* for $k_{max} \geq 16$.

While the observed speedups are impressive, the significance of our contribution becomes even more clear, if we look at the runtime from a different perspective. Figure 7 shows the ratio of the runtime to compute k_{max} MSTs over the runtime to compute a single MST. RNG* exhibits a very stable ratio of about 2 for all values of k_{max}, *i.e*, we can use it to compute as many as 128 MSTs/hierarchies for the computational cost of naively computing about 2 MSTs/hierarchies.

VI. CONCLUSION

We presented an efficient strategy for computing multiple density-based clustering hierarchies. We formally showed that the use of the Relative Neighborhood Graph as a substitute for the Mutual Reachability Graph is advantageous when one wants to explore state-of-the-art HDBSCAN* solutions w.r.t. multiple values of $mpts$, while ensuring theoretical correctness of results. Our experiments showed that the proposed method can be significantly faster than a baseline strategy based on running HDBSCAN* exhaustively (yet in an optimized way) for different values of $mpts$. In particular, it scales considerably better when running on large datasets and more prominently for broader ranges of $mpts$ values.

In our future work we intend to investigate strategies to simultaneously explore, visualize and possibly combine the whole spectrum of clustering solutions that are available both across multiple hierarchies (corresponding to different values of $mpts$) as well as across different hierarchical/density levels, taking into account the quality of these solutions according to different unsupervised criteria.

REFERENCES

[1] P. K. Agarwal and J. Matousek. Relative neighborhood graphs in three dimensions. *Computational Geometry*, 1992.
[2] M. Ankerst, M. M. Breunig, H. Kriegel, and J. Sander. OPTICS: ordering points to identify the clustering structure. In *SIGMOD*, 1999.
[3] P. B. Callahan. *Dealing with higher dimensions: the well-separated pair decomposition and its applications.* PhD thesis, 1995.
[4] P. B. Callahan and S. R. Kosaraju. A decomposition of multidimensional point sets with applications to k-nearest-neighbors and n-body potential fields. *Journal of the ACM*, 1995.
[5] R. J. G. B. Campello, D. Moulavi, and J. Sander. Density-based clustering based on hierarchical density estimates. In *PAKDD*, 2013.
[6] R. J. G. B. Campello, D. Moulavi, A. Zimek, and J. Sander. Hierarchical density estimates for data clustering, visualization, and outlier detection. *TKDD*, 2015.
[7] G. Cattaneo, P. Faruolo, U. F. Petrillo, and G. F. Italiano. Maintaining dynamic minimum spanning trees: An experimental study. *Discrete Applied Mathematics*, 2010.
[8] X. Chen, Y. Min, Y. Zhao, and P. Wang. GMDBSCAN: multi-density DBSCAN cluster based on grid. In *ICEBE*, 2008.
[9] B. Delaunay. Sur la sphère vide. A la mémoire de Georges Voronoï. *Bulletin de l'Académie des Sciences de l'URSS*, 1934.
[10] M. Ester, H. Kriegel, J. Sander, and X. Xu. A density-based algorithm for discovering clusters in large spatial databases with noise. In *KDD*, 1996.
[11] K. R. Gabriel and R. R. Sokal. A new statistical approach to geographic variation analysis. *Systematic Biology*, 1969.
[12] J. Handl and J. Knowles. Cluster generators for large high-dimensional data sets with large numbers of clusters, 2005.
[13] M. R. Henzinger and V. King. Maintaining minimum spanning trees in dynamic graphs. In *ICALPS*, 1997.
[14] A. Hinneburg and D. A. Keim. An efficient approach to clustering in large multimedia databases with noise. In *KDD*, 1998.
[15] G. A. II, G. Cattaneo, and G. F. Italiano. Experimental analysis of dynamic minimum spanning tree algorithms (extended abstract). In *ACM-SIAM Symposium on Discrete Algorithms*, 1997.
[16] J. W. Jaromczyk and G. T. Toussaint. Relative neighborhood graphs and their relatives. *Proceedings of the IEEE*, pages 1502–1517, 1992.
[17] A. Karami and R. Johansson. Choosing dbscan parameters automatically using differential evolution. *IJCA*, 2014.
[18] D. G. Kirkpatrick and J. D. Radke. A framework for computational morphology. 1984.
[19] L. Lelis and J. Sander. Semi-supervised density-based clustering. In *ICDM*, 2009.
[20] D. W. Matula and R. R. Sokal. Properties of gabriel graphs relevant to geographic variation research and the clustering of points in the plane. *Geographical Analysis*, 1980.
[21] D. Moulavi, P. A. Jaskowiak, R. J. G. B. Campello, A. Zimek, and J. Sander. Density-based clustering validation. In *SDM*, 2014.
[22] A. Smiti and Z. Elouedi. Dbscan-gm: An improved clustering method based on gaussian means and dbscan techniques. In *INES*, 2012.
[23] G. T. Toussaint. The relative neighbourhood graph of a finite planar set. *Pattern Recognition*, 1980.
[24] J. Wetherell. Java: Algorithms and data structure. Available at https://github.com/phishman3579/java-algorithms-implementation.